2010 IEEE International Conference on Robotics and Automation
Anchorage Convention District
May 3-8, 2010, Anchorage, Alaska, USA

Myometry-Driven Compliant-Body Design for Underwater Propulsion

O. Akanyeti[1], A. Ernits[2], C. Fiazza[1], G. Toming[2], G. Kulikovskis[3],
M. Listak[2], R. Raag[2], T. Salumäe[2], P. Fiorini[1], M. Kruusmaa[2]

Abstract— **Within the broader scope of underwater biomimetics, in this paper we address the relevance of factors such as shape and elasticity distribution in the ability of a compliant device to imitate the kinematic behaviour of a fish. We assess the viability of myometry as a tool to determine candidate mechanical parameters without relying solely on analytical models; we show that we can obtain elasticity distributions that are both consistent with previous theoretical investigations and experimentally better adherent to the passive kinematics of a biological embodiment (rainbow trout).**

I. INTRODUCTION

The overall goal of our work is to design a biomimetic underwater propulsion system with higher power-thrust efficiency and maneuverability than current underwater vehicles. The biological inspiration is steadily swimming fish. In order to reproduce the dynamics of a fish during its steady swimming, in particular sub-carangiform swimming in rainbow trouts, we first study its structural morphology. Our starting point is assessing the properties of the device's structure, examining in particular the following three questions:

1) Which characteristics of fish morphology enable fish to achieve high swimming performances?
2) Which mechanical design approach is most suited to develop an underwater vehicle with similar characteristics?
3) In the chosen approach, which design parameters are most relevant? What methodology can we successfully employ to determine values for such parameters?

The first question is answered in literature. Previous research on fish swimming ([1], [2], [3], [4], [5]) stresses the importance of few key features in achieving high swimming efficiency: i) undulating motion mechanics, in which a body wave travels downstream with phase speed greater than the fish's swimming speed; ii) the ability to alter the body wave speed, by adjusting tail beat frequency and/or body wavelength; iii) the ability to tune the body wave in terms of amplitude and phase.

In light of this set of competences, we address the following question "What is the simplest mechanical design that can accomplish this overall functionality?". Traditionally, robots that mimic fish ([6], [7], [8]) are built with rigid components connected by joints. This design style leads to complex mechanisms with inevitable controllability difficulties.

[1]Dept. of Computer Science, University of Verona, Italy
[2]Center for Biorobotics, Tallinn University of Technology, Estonia
[3]Dept. of Theoretical Mechanics, Riga Technical University, Latvia

A. Modelling fish as visco-elastic bodies

We have decided to use the visco-elastic compliant-body approach recently proposed in [9]. This approach is inspired by [10], in which the body of a real fish is modeled as a visco-elastic beam. In this approach, devices are compliant continuous flexible bodies, in which material distribution allows a minimal set of input functions to exploit resultant modes of vibration for locomotion.

Locomotion-inducing waves travelling along the elastic body are achieved through phase differences between subsequent points in the body; phase depends on viscosity and timing is critical. Hence, two important design parameters emerge in affecting device performance: spatial distribution of elasticity and of viscosity. These design parameters encapsulate i) geometry of the body (shape and size), ii) material distribution along the body, and iii) visco-elastic characteristics of each constituent material.

1) Analytical Approach: A promising way of computing these parameters is through analytical models. The standard model for fish comes from slender-body theory ([1]), which has been developed for small displacements but can be extended further. In recent studies ([10], [11]), the fish body has been modeled as a visco-elastic beam and analyzed in the domain of Euler-Bernoulli/Timoshenko beam theory. Lateral motion is described by the solution of the partial differential equation (PDE) associated to the visco-elastic beam. Given a geometry, the desired kinematics and the set of available actuation signals, a PDE model can relate prototype behavior to the target parameters. For simple geometries and uniform material distributions these equations can be solved to obtain reliable values ([12]). Moreover, PDE models can be used to determine favorable operating conditions — such as optimal operational range of frequencies and position of the excitation point.

However, PDE models, in general, suffer from an enormous increase in computational complexity with increasing dimensionality. As the number of parameters increases for geometries with tail, fins and non-uniform material distributions, the models get more complex and it is extremely difficult to solve their characteristic equations. This leads to over-simplified models which perform poorly when compared to biological fish.

2) A myometry-based approach: In this paper, we propose an alternative method and test its viability. We wish to obtain design parameters from direct investigation of real fish bodies. For direct analysis, we perform myometry on fish. Myometry is a method for non-invasive measurement of biomechanical properties of the muscles; myometry data

can enable us to better understand how the visco-elastic properties of fish muscles change along the body. If successful, this method allows bypassing analytical difficulties. In this paper, we focus in particular on the elastic properties of fish; we attempt to identify the elasticity distribution and employ it as values for soft-bodied robot design.

The main benefits of the proposed design method are: i) It is a simple, fast and efficient method for computing the desired modelling parameters. ii) It requires few theoretical assumptions. This enables us to design more realistic models with complex shapes and non-uniform material distributions. iii) Moreover, the method can be used to crossvalidate the analytical modelling approach and complement it; for instance, findings from myometry can be used as boundary conditions for analytical models or to reduce the dimensionality of unknown model parameters.

B. Paper methodology

Our methodology can be decomposed into four phases:

1) We perform myometry on biological specimens, measuring muscle properties along the body. We derive estimates for the elasticity distribution for real fish.
2) On the basis of geometry and estimated elasticity, we estimate the target properties of our biomimetic device: geometry, material properties, material distribution.
3) We manufacture prototypes for comparative experiments; prototypes vary in elasticity, elasticity distribution and geometry.
4) We conduct experiments to verify the kinematics of the prototypes against a real trout. We assess the kinematic similarity between prototype performance and real fish. We describe similarity by correlating body bending; we also evaluate the differences in point-wise displacement.

II. FISH MYOMETRY

To perform myometry we employ a Myoton, a device developed by Müomeetria AS. ([13]). The device operates by locally stimulating the tissue with a small impact and recording the resulting dampening oscillation through an accelerometer. A microprocessor analyzes the signals to output tone (frequency of the oscillation in Hz), logarithmic decrement (logarithm of the ratio of consecutive peaks) and stiffness of the tissue (in N/m) ([14]). Tone characterizes muscle tension, whereas decrement quantifies a muscle's ability to restore its initial shape after contraction. Stiffness refers to the muscle's resistance to changes in shape due to external forces.

Myometry is generally used to measure human skeletal muscles ([15]-[16]). In measuring relatively smaller-sized muscles (such as fish muscles), we expect that the Myoton readings do not depend solely on local muscle properties, but up to a certain distance ("the effective depth") also on the neighboring materials along the direction of the applied force (Figure 1). However, so far no data is available in the literature to establish with precision what the effective depth is. When tested on a homogeneous material with varying thickness, the myometer's stiffness readings are found to be affected by the width at the point of measurement. We can consider the myometer readings k in terms of an "equivalent stiffness": $k = \frac{EA}{w(x)}$, where E is Young's modulus, A is the area associated to the applied force and $w(x)$ is the width at the point of measurement. We have also tested the myometer on a homogeneous cone with known elasticity, and compared myometer readings with the theoretical values for elasticity. We found that the myometer follows

$$k = \alpha(x)\frac{EA}{w(x)}, \tag{1}$$

where $\alpha(x)$ is a scaling coefficient with value approximately 0.5, and that adherence to theoretical values is poor when material thickness is very small (sensibly less than 5 cm). In terms of fish measurements, this means that fish is in the range of reliable thickness in the central section (see Figure 2, regions $R1 - R4$).

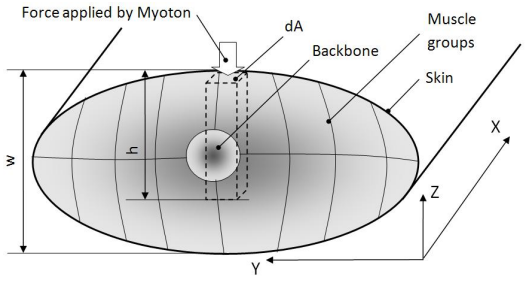

Fig. 1. Cross sectional view of fish body during myometry.

A. Experiments with Trout

For myometry experiments we used two fresh-water trouts. One fish measured approximately 40cm and the other approximately 50cm in length. Myometry was performed shortly after death, to minimize intervening changes in muscle properties. During measurements, the specimen were placed on a soft pillow-like surface. For each fish, we chose 25 sample points, to cover the surface of the body in the regions of interest. Sampling points are grouped in 5 regions (from midsection ($R1$) to tail ($R5$)), each containing 5 measurement points; each measurement was repeated 10 times. Figure 2 shows location of the sampling points for the second specimen. We take measurements only on 5 points per region to contain the duration of the myometry experiments, to avoid changes in stiffness due to rigor mortis.

B. Results and Analysis

Table I summarizes myometry data and elasticity estimates. Figure 3 shows that in fish E increases towards the tail. The measurements in Region 5 should be considered less reliable because the width is very small and interference from the underlying material is not negligible.

We believe the increase in E is related to the decrease in muscle-bone ratio of the body — as we approach the tail, the relative effect of bones on stiffness measurements increases.

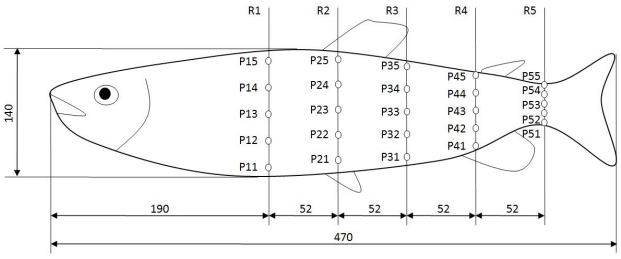

Fig. 2. Measurement points in myometry experiments (fish 2)

TABLE I

MYOMETRY READINGS AND ELASTICITY ESTIMATES.

	log. dec.	freq. $(1/s)$	stiff. (N/m)	elas. (KPa)
Fish 1				
R1	2.1 ± 0.1	15.4 ± 0.9	347.8 ± 18.4	222.6
R2	2.2 ± 0.1	16.9 ± 0.5	359.4 ± 24.8	224.8
R3	2.4 ± 0.1	19.0 ± 0.5	414.5 ± 26.5	275.7
R4	2.7 ± 0.1	21.4 ± 1.0	422.0 ± 19.7	478.3
R5	2.8 ± 0.1	13.4 ± 0.6	340.0 ± 17.7	618.5
Fish 2				
R1	1.4 ± 0.2	22.0 ± 2.6	466.9 ± 57.1	247.9
R2	1.2 ± 0.2	23.7 ± 2.4	519.7 ± 53.3	285.0
R3	1.2 ± 0.2	25.7 ± 2.3	569.9 ± 54.1	370.9
R4	1.3 ± 0.2	31.3 ± 1.9	629.1 ± 22.1	610.3
R5	2.2 ± 0.1	35.8 ± 2.4	505.0 ± 24.6	703.2

As bone is stiffer than muscles, E locally increases. Moreover, near the tail muscles are more tightly packed and there is more cartilage and tendon at the tail. This is also coherent with the theoretical models described in [10].

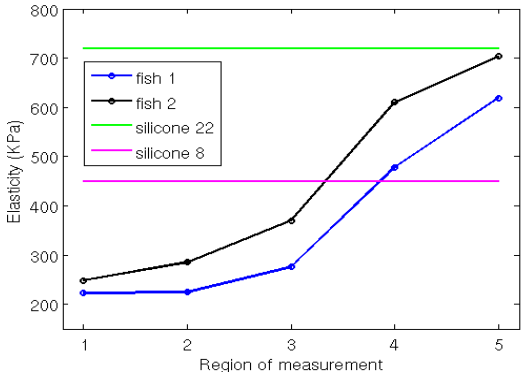

Fig. 3. Elasticity distributions of two fish. Elasticity values for two silicone materials are also plotted. Both materials are used during manufacturing prototypes (see Section III).

III. COMPLIANT-BODY DESIGN

Using myometry data, we have thus identified a candidate distribution of elasticity for our biomimetic device (figure 3). Direct investigation of fish has provided information on both a desirable trend – increase E towards the tail – and a desirable value for average elasticity.

The next step is to identify materials whose Young's modulus lies in the biological range. We employ silicone-based materials Elite Double 8 (E8, Shore A scale: hardness of 8, elasticity $450KPa$) and Elite Double 22 (E22, Shore A scale: hardness of 22, elasticity $720KPa$). Figure 3 shows the elasticity values of the two silicone materials along with the biological distributions obtained via myometry. E8 lies in the middle of the biological range (200-700 KPa) and can be considered representative of the average elasticity of fish, whereas E22 approximates the highest value measured in fish.

TABLE II

GEOMETRY, LENGTH (L) AND ELASTICITY (E) VALUES FOR MANUFACTURED PROTOTYPES. ELASTICITY VALUES: $E_1 = 454.4KPa$ AND $E_1 = 722.0KPa$. SHAPES: CYLINDER (A), ELLIPTICAL TRUNCATED CONE (B) AND FISH-LIKE (C). GEOMETRY: r_1 AND r_2 ARE MAJOR AND MINOR RADII FOR THE ELLIPTICAL CROSS SECTION AT THE LARGEST EXTREMITY.

Prot. #	E (Pa)	Shape	L (cm)	Geometry (cm)
P1	E_1	A	25	$r_1 = 4.5, r_2 = 2.25$
P2	E_2	B	25	$r_1 = 6, r_2 = 3$
P3	E_1	B	25	as P2
P4	E_2	C	30	as P2
P5	E_1	C	30	as P2
P6	E_1, E_2	C	30	as P2

The goal of our experimental procedure is assessing the passive kinematic similarity of biomimetic devices with respect to a fish body. For comparative experiments, we employ three different geometries (cylinder, truncated elliptical cone and elliptical cone with tail).

Prototype P1 is a cylinder made of E8. This prototype is used as analytical reference, because a solved partial differential equation describing its dynamics is available in [9]. Prototypes P2 and P3 (made of E22 and E8, respectively) are designed as elliptical truncated cones. This geometry can be seen as intermediate in complexity between a cylinder and a realistic fish-shape. Prototypes P4 to P6 are elliptical cones terminating with a tail ("fish-shaped" prototypes). Prototypes 4 and 5 are made from E22 and E8, respectively. To approximate an increasing elasticity distribution and mimic the trend found from myometry, prototype P6 is hybrid: the first part of the body is made of E8 and the posterior section, tail included, is fabricated out of E22. See Table II for physical properties of prototypes displayed in Figure 4. In total, we have 6 prototypes available for comparative experiments — with varying elasticity, elasticity distribution and geometry.

A. Fabrication of Prototypes

The manufacturing process comprises two steps: mould making and casting. For truncated elliptical cone-shaped bodies, a positive mould was cut out of expanded polystyrene (EPS) using electrically heated wire. After smoothing the surface with polyvinyl acetate (PVA) glue, the positive mould was covered with glass fiber cloth and painted with epoxy resin to obtain the negative mould. More complex moulds were milled on a computer numerical controlled (CNC) machine. As the silicone we used is virtually impossible to

Fig. 4. Compliant prototypes used in the experiments. The prototypes are manufactured using two different silicone materials: i) Elite Double 22 (green) and Elite Double 8 (pink). The elasticity values for E8 and E22 are, respectively, around 450KPa and 720KPa.

TABLE III

AVERAGE SPEARMAN RANK CORRELATION AND AVERAGE DIFFERENCE IN LATERAL DISPLACEMENT. LEFT: ACROSS ALL TEST SCENARIOS; RIGHT: AVERAGED FOR FREQUENCIES IN THE 1-4 HZ RANGE. 5 HZ IS NOT IN THE BIOLOGICAL RANGE OF ACTUATION.

	All tests		Reduced range (1-4 Hz)	
	Spr.	Lmd.	Spr.	Lmd
P1	0.29 ± 0.06	9.11 ± 0.35	0.33 ± 0.06	9.15 ± 0.38
P2	0.36 ± 0.05	13.76 ± 0.60	0.36 ± 0.06	13.83 ± 0.66
P3	0.22 ± 0.07	13.41 ± 0.74	0.29 ± 0.06	13.62 ± 0.84
P4	0.63 ± 0.05	5.97 ± 0.46	0.68 ± 0.04	6.10 ± 0.56
P5	0.65 ± 0.06	3.99 ± 0.12	0.73 ± 0.04	3.98 ± 0.15
P6	0.71 ± 0.06	3.94 ± 0.18	0.77 ± 0.05	3.95 ± 0.22

glue or fix with screws after curing, actuator mounts were inserted into the moulds during casting. The mounts are rigid plates with threaded holes for mounting and holes or pores to form a strong interface with silicone.

IV. COMPARATIVE EXPERIMENTS

A. Experimental Setup

The experiments were conducted in the flow tank of Tallinn University of Technology. The size of the tank is (4x1.5x1.5)m^3, with working section volume (0.5x0.5x1.5)m^3 and cross sectional area (0.5x0.5)m^2. The tank is aerated and powered with an electric motor to generate a laminar water flow. The tank is equipped with a Doppler sonar velocity log system to measure the laminar flow speed.

We tested all 6 prototypes (Figure 4) and one rainbow trout (*Oncorhynchus mykiss*), immediately after death. Test objects were oriented with their main axis along $\hat{x}$ and up along $\hat{z}$ – with gravity lying in $-\hat{z}$. Objects were supported using a vertical rod along $\hat{z}$ and a rotational joint. A waterproof DC-motor was used to actuate the body in the transverse direction (xy-plane). The applied torque was a sinusoidal signal with fixed amplitude (1Nm). Each object was tested in three flow conditions: static water and two laminar flows, with speeds $0.25ms^{-1}$ and $0.5ms^{-1}$. The static water regimen serves as a reference condition, as the corresponding equations have already been analyzed [11], whereas the highest laminar flow speed is close to the cruising speed of rainbow trouts.

For each flow condition, each prototype was tested under applied torques of different frequencies (1-5 Hz). This corresponds to 105 experiments in total. In all cases, we tracked the kinematics of the models for approximately 30 seconds. Movement was captured by an overhead camera recording the test object against a lighted background. The camera images were logged with frame rate 60 Hz; images were postprocessed to obtain point-wise lateral displacement, bending curvature, phase velocity and bending moment distribution for each test object. Figure 5 shows two sets of sample images (a trout and the hybrid prototype P6), recorded in static water with operating frequency 1 Hz.

In order to generate a good design for our biomimetic device, we investigate if tuning elasticity distribution and geometry can bring the prototype closer in behaviour to our biological reference. Better adherence to the passive kinematics of the trout is considered better performance. Correlation between the prototypes and the reference specimen with respect to kinematic characteristics can verify if our myometry-based design method is a useful tool. We use Spearman rank correlation coefficients to relate the bending performance of prototypes to fish (curvature distribution); we also measure the difference in lateral displacement between prototypes and fish and evaluate the mean absolute lateral motion difference.

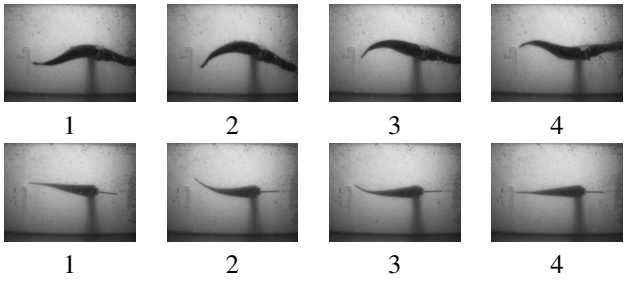

Fig. 5. Two sets of images captured by overhead camera (xy-plane) during experiments in static water at 1Hz. First row: rainbow trout; second row: hybrid prototype (P6). The time interval between consecutive snapshots in the set is 100ms.

B. Results

a) Complex interplay between geometry and elasticity: Figure 6 presents Spearman rank correlation coefficients and mean position difference. In Table III we summarize performance results across the 15 test conditions. In all test scenarios, prototypes with fish-like geometry (P4, P5 and P6) perform significantly better than the rest. However, contrary to our expectation, cone-shaped prototypes did not perform better than the cylinder; the cylinder outscores both P2 and P3 consistently on error and P3 also on correlation. Thus, geometry is an important factor in achieving fish-like swimming, although by itself it cannot predict relative performance. The principle that, as geometry gets closer to the geometry of fish, performance does too, does not necessarily hold even if elasticity is not allowed to vary.

We also observe that the hybrid prototype (P6) performed slightly better than P4 and P5. P6 has the highest number of

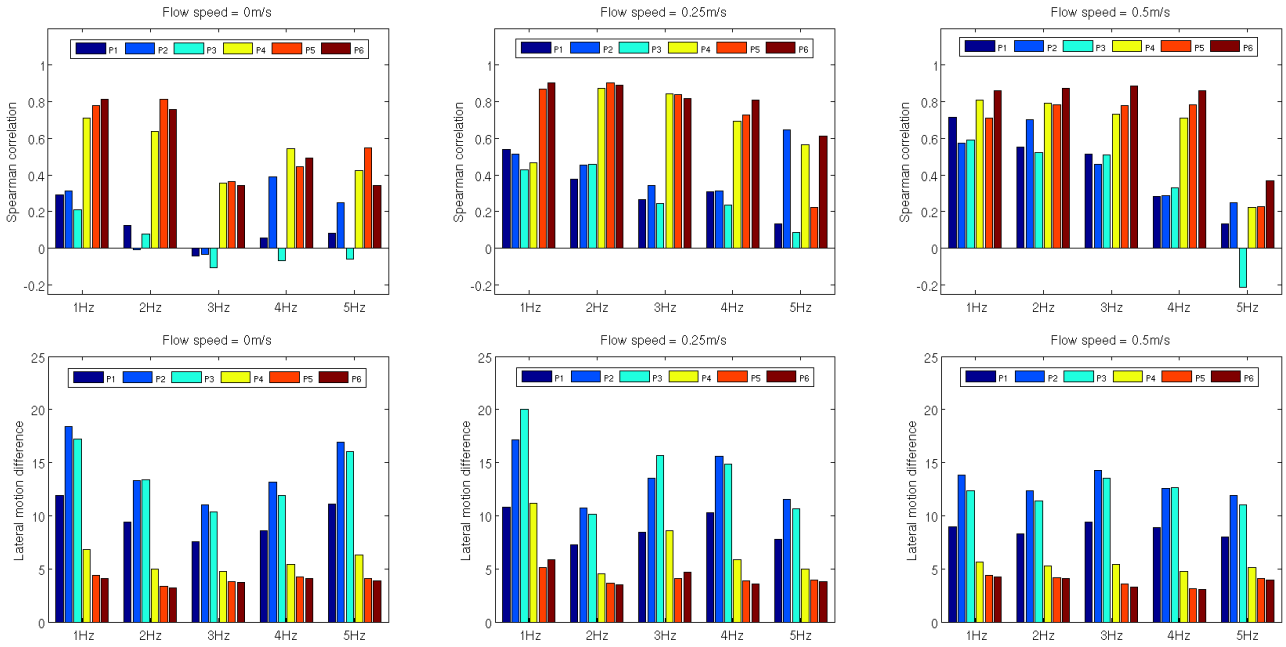

Fig. 6. Experimental results. Row 1: Spearman rank correlation (similarity in bending behaviour), all correlation coefficients presented in graphs are statistically significant ($p < 5\%$). Row 2: lateral motion difference (dissimilarity in amplitude behaviour).

best performances for both similarity criteria (8 w.r.t curvature and 10 w.r.t amplitude). Non-negligible improvement (6-8% across all tests and 4-9% in the reduced 1-4 Hz range) arises even from a crude 2-value approximation to the experimentally determined elasticity distribution. This confirms that designing compliant prototypes with varying elasticity is a key technology for biomimesis of fish.

Turning attention to the role of average elasticity, we now consider prototypes with the same shape. The soft fish (P5) performs better than the hard fish (P4), but the hard cone (P2) performs better than the soft cone (P3). This contradicts the expectation that a change in average elasticity affects all shapes in the same manner. Also, the principle that, as average elasticity gets closer to the elasticity of fish, performance does too, does not necessarily hold even if shape is not allowed to vary. All these observations suggest a complex relationship between geometry and elasticity.

b) Fish torso is overdamped beyond 3Hz in static water: In static water, the similarity between prototypes and real fish decreases with increasing input frequency. The phenomenon is more evident after $3Hz$. The kinematic behaviour of fish changes distinctly after $3Hz$; the anterior part of the body hardly bends and bending amplitude increases very slowly towards the tail. Figure 7 illustrates the bending motions of the fish body at two different frequencies ($1Hz$ and $4Hz$). The results are coherent with previous research reporting that the fish body is overdamped at high frequencies ([10]). Although the natural frequency of the prototypes is in the range of the fish's natural frequency, no such overdamping is observed for prototypes. At higher frequency, the overall type of motion does not change for prototypes aside from the obvious reduction in amplitude. This observation suggests that fish are mechanically engineered to operate at lower frequencies and this feature does not rest solely on geometry but requires tuning elasticity and viscosity distribution along the body. Overdamping of this sort can be observed also for experiments in laminar regimen, although the trend is far less clear than in still water.

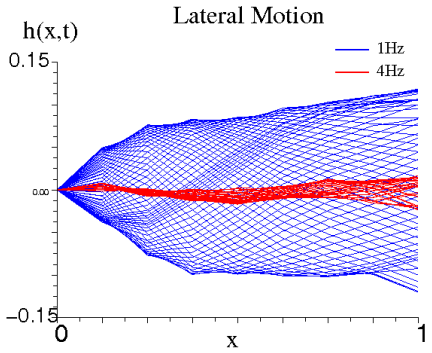

Fig. 7. Lateral motion h(x,t) of a trout body at $1Hz$ (blue) and at $4Hz$ (red). Note that at $4Hz$ the body torso hardly bends.

c) Observations on Passive Bending Moments: We now examine the distribution of the elastic bending moment M_E in fish and fish shaped prototypes (P4, P5 and P6). M_E is obtained as $M_E = EI\frac{\partial^2 h(x,t)}{\partial x^2}$ and is shown in Figure 8 for one cycle in static water at $1Hz$. M_E decreases gradually and approaches zero at two thirds of the body length. This trend is consistent with the reduction in passive visco-elastic bending moments predicted in [10], except for position of the peak amplitude for M_E. In free swimming fish, the peak amplitude is just before the mid-part of the body, whereas

in our case M_E is highest at the origin. This is due to the actuation style: in our experiment the fish body is subject to sinusoidal torque input at one extremity. In other words the boundary conditions are not the same: $M(0) \neq 0$. This shows that favorable effects arise in the hydrodynamic moment even when actuation is localized. Moreover, in prototypes there is a lateral asymmetry in the distribution of elastic bending moments, which is completely absent in the biological reference. Asymmetry seems to stem from the actuated extremity, so it might be possible that the phenomenon is at least partly originated by the fact that prototypes lack a head.

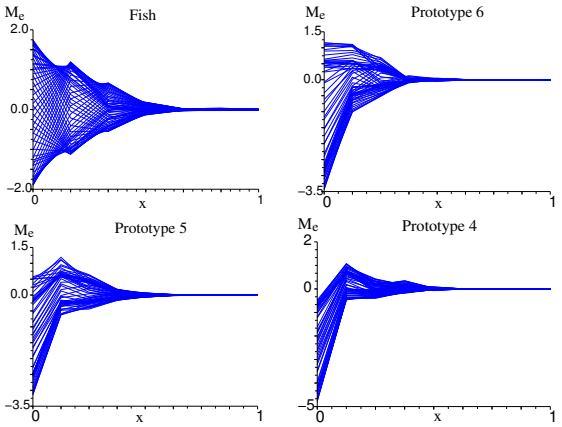

Fig. 8. The elasticity bending moment distribution ($M_E(x)$) along the body (x) of fish and fish-shaped prototypes (P4, P5 and P6). The experiments were conducted in static water at $1Hz$.

V. Conclusions

In this paper, we conduct comparative experiments to investigate the relevance of factors such as geometry and elasticity, in a visco-elastic body's ability to imitate the kinematics of real fish. We also test the viability of myometry in orienting the design of biomimetic devices. The outcomes of our experiments are listed below:

Myometry is an interesting tool and can be used to obtain more information about the biomimetic reference that we are trying to mimic. In particular, we demonstrate this fact by estimating the elasticity distribution of biological fish.

There is a complex relationship between geometry and stiffness. Tuning one of them independently from the other does not always guarantee an improvement in performance. This limits the application of heuristic design methods — based on trial and error processes — and suggests that formal design methodologies, such as using myometry, are needed to optimize our biomimetic devices.

The torso in fish is overdampened after 3 Hz. This indicates that the viscosity distribution plays an important role in regulating bending moments along the fish body. It also suggests that the structure itself generates stability for swimming. Therefore, if the task is to replicate efficient fish swimming, a noticeable component of stabilization derives from the embodiment itself. We expect that the task of control shall not be entirely in charge of guaranteeing stability.

The hybrid prototype performed better than other fish-shaped prototypes. We believe that it is the increasing elasticity that grants P6 an edge.

Future Work: To approximate the elasticity distribution of fish we manufactured the body of the hybrid prototype (P6) in two sections using two different materials. This is a crude 2-value approximation and the performance is affected by the discontinuity. We are, therefore, investigating ways of designing prototypes with continuously-varying elasticity. We are also examining the following question: "how can myometry readings be used to improve and/or simplify the analytical models?". We are looking for ways of employing myometry with live fish and working on developing a simple method to estimate the viscosity distribution from myometry experiments.

VI. Acknowledgements

This work is carried out under the FILOSE project, supported by the European Union, seventh framework programme (FP7-ICT-2007-3).

References

[1] M. J. Lighthill, Note on the swimming of slender fish, *Journal of FluidMech*, 1960, vol. 9, 305-317.
[2] M. J. Lighthill, Large Amplitude Elongated Body Theory of Fish Locomotion, *Proceedings of the Royal Society, Biological Sciences*, vol. 179, 1971, pp. 125-138.
[3] F. Hess, and J. J. Videler, Fast Continuous Swimming of Saithe (Pollachius Virens): A Dynamical Analysis of Bending Moments and Muscle Power, *Journal of Experimental Biology*, vol. 109, 1984, pp. 229-251.
[4] M. S. Triantafyllou, and G. S. Triantafyllou, and D. K. P. Yue, Hydrodynamics of Fish-like Swimming, *Journal of Fluid Mechanics*, 2000, vol. 32, pp. 33-55.
[5] George V. Lauder and Peter G. A. Madden, Learning from Fish: Kinematics and Experimental Hydrodynamics for Roboticists, *International Journal of Automation and Computing*, vol. 4, 2006, pp. 325-335.
[6] Michael S. Triantafyllou, and George S. Triantafyllou, An Efficient Swimming Machine, *Scientific American*, vol. 272:3, 1995, pp. 272-3.
[7] D. S. Barrett, M. S. Triantafyllou, D. K. P. Yue, M. A. Grosenbaugh, and M, J. Wolfgang, Drag Reduction in Fish-like Locomotion, *Journal of Fluid Mechanics*, vol. 392, 1999, pp. 183-212.
[8] J. Liu and H. Hu. Novel Mechatronics Design for a Robotic Fish. *IEEE/RSJ International Conference on Intelligent Robots and Systems (IROS)*, Edmonton, Canada, 2005, pp. 2077-2082.
[9] Pablo Valvidia y Alvarado, Design of Biomimetic Compliant Devices for Locomotion in Liquid Environments, *Ph.D. Thesis*, MIT, 2007.
[10] J. Y. Cheng, T. J. Pedley and J. D. Altringham, A Continuous Dynamic Beam Model for Swimming Fish, *Philosophical Transactions of the Royal Society B: Biological Sciences*, vol. 353, 1998, pp. 981-997.
[11] Pablo Valdivia y Alvarado, and Kamal Youcef-Toumi, Design of Machines With Compliant Bodies for Biomimetic Locomotion in Liquid Environments, *Journal of Dynamic Systems, Measurement and Control*, vol. 128, 2006, pp. 3-13.
[12] Brenden P. Epps, Pablo Valdivia y Alvarado, Kamal Youcef-Toumi, and Alexandra H. Techet, Swimming Performance of a Biomimetic Compliant Fish-like Robot, *Experimental Fluids*, 2009.
[13] Müomeetria AS., Myoton:Inventions for Performance, available at *www.myoton.ee*.
[14] Zenija Roja, Valdis Kalkis, Arved Vain, Henrijs Kalkis, and Maija Eglite, Assessment of skeletal muscle fatigue of road maintenance workers based on heart rate monitoring and myotonometry, *Journal of Occupational Medicine and Toxicology*, vol: 1:20, 2006, pp. 1-9.
[15] Georg Gavronski, Alar Veraksit, Eero Vasar, and Jaak Maaroos, Evaluation of viscoelastic parameters of the skeletal muscles in junior triathletes, *Physiological Measurement*, vol. 28, 2007, pp. 625-637.
[16] Mario Bizzini, and Anne F. Mannion, Reliability of a new, hand-held device for assessing skeletal muscle stiffness, *Clinical Biomechanics*, vol. 18, 2003, 459-461.